Received 14 June 2021; revised 14 July 2021; accepted 15 July 2021. Date of publication 21 July 2021; date of current version 4 August 2021.

Digital Object Identifier 10.1109/OJAP.2021.3098947

Dual-Resonant High-Gain Wideband Yagi-Uda Antenna Using Full-Wavelength Sectorial Dipoles

WEN-QI JIA[1], FEI-YAN JI[1], WEN-JUN LU[1] (Senior Member, IEEE), CHEN-XIN PAN[1], AND LEI ZHU[2] (Fellow, IEEE)

[1]Jiangsu Key Laboratory of Wireless Communications, College of Communications and Information Engineering, Nanjing University of Posts and Telecommunications, Nanjing 210049, Jiangsu, China

[2]Faculty of Science and Technology, University of Macau, Macau, China

CORRESPONDING AUTHOR: W.-J. LU (e-mail: wjlu@njupt.edu.cn)

This work was supported in part by the National Natural Science Foundation of China under Grant 61871233, Grant 61427801, and Grant 61471204, and in part by the Postgraduate Research and Practice Innovation Program of Jiangsu Province under Grant KYCX20_0808.

ABSTRACT A novel design approach to high-gain, wideband, dual-resonant, closely-spaced, three-element Yagi-Uda antenna is advanced. The antenna is comprised by a full-wavelength, principal sectorial dipole, a circular metallic flat reflector, and a sectorial director. At first, a multi-source model is developed to predict the initial values of the key antenna parameters, e.g., the flared angle/radius of the director, and the separation between them. Then, as theoretically predicted, numerically simulated and experimentally validated, the flared angles of the principal radiator and the director are eventually determined as 270° and 180°, respectively. They are further tightly coupled at a close separation of 0.024-wavelength to yield relatively compact size and high gain simultaneously. Prototype antenna with a circular metallic reflector successfully exhibits an impedance bandwidth up to about 40%, with in-band maximum gain up to 10.4 dBi and gain fluctuation less than 3 dB. Finally, the antenna is comparatively studied with other Yagi-Uda antennas to highlight its unique wideband and high gain characteristics.

INDEX TERMS Wideband antenna, Yagi-Uda antenna, full-wavelength dipole antenna, dual-mode resonance, high gain antenna.

I. INTRODUCTION

WITH the rapid development of wireless communication technology, there is a growing demand for antennas with high performances. Yagi-Uda antennas enjoy many advantages over conventional elementary antennas, such as high gain/directivity, easy to set up, and low cost. Since invented in 1926 [1], variants of Yagi-Uda antennas have been extensively developed and presented [2]–[4]. Up to now, Yagi-Uda antennas can be basically classified into four distinctive types. The first one should be the fundamental type [5], which are composed of a principal dipole, a reflector, and some directors that resonating at their respective half- wavelength mode with linear polarization. Typically and empirically, the directors and the principal dipole are coupled at a distance between 0.1-wavelength and 0.3-wavelength [5]. Modified Yagi-Uda antennas, e.g., curved Yagi-Uda antenna [6], origami antennas [7], those with special reflectors [8]–[9], compact designs [3], [10]–[16], etc, can be recognized as the second type. Dipole shaping technique can yield improved performance as expected, such as directivity enhancement [6]–[7], [13], high front-to-back ratios [8]–[9], broadband operation [7], [10]–[11], size miniaturization [11]–[16], etc. The "array technique" can be recognized as the third type design approach to further performance enhancements [16]–[22], e.g., higher efficiency [16]–[18], more compact size [17] and better directivity [19]–[22]. Such Yagi-Uda arrays with enhanced performances have been widely applied in satellite communications [16], vehicle communications [16], [23], millimeter-wave

communications [24]–[26], radar systems [27], etc. The fourth type is the printed-circuit board (PCB) Yagi-Uda antennas, which is also generally called as "quasi-Yagi antennas" [28]–[34]. Quasi-Yagi antennas have several advantages over the traditional ones: The presence of dielectric substrate can provide its attractive ability in mechanical support of the antenna and on-chip integrability with planar feeding circuits as well, which may bring the merit of easy fabrication.

Basically and typically, the reflector, director and radiator of Yagi-Uda antennas are 1-D, half-wavelength dipoles, where two adjacent ones are closely spaced at a separation between 0.1-wavelength to 0.3-wavelength. To our best knowledge, there are no reported Yagi-Uda antennas, which are comprised by full-wavelength dipoles, so far. Recent studies have revealed that both 1-D and 2-D full-wavelength dipoles [35]–[38] can exhibit better performance than the half-wavelength dipole, such as wider bandwidth [35], [38], higher gain [36]–[37], and improved polarization purity within the whole beamwidth [38]. Therefore, it is highly expected that a novel class of wideband, high gain Yagi-Uda antennas can be presented, designed and implemented by using multi-resonant, 2-D full-wavelength sectorial dipoles [38].

In this paper, a novel design approach to high-gain, dual-mode resonant, closely-spaced, three-element Yagi-Uda antenna is advanced based upon 2-D full-wavelength sectorial dipoles. The antenna is composed of a full-wavelength, principal sectorial radiator, a circular metallic flat reflector, and a full-wavelength sectorial director [38]. At first, a multi-source model is developed to calculate the initial parameters of the antenna. Through numerical simulations, the design parameters can be finely tuned and properly determined. Then, the antenna prototypes are fabricated and measured to verify design approach. In final, the performance of the antenna is further improved by adjusting the size of the ground plane.

II. PRINCIPLE AND DESIGN APPROACH

A. EQUIVALENT SIX-SOURCE MODEL

The design procedure initiates from a full-wavelength, 2-D sector principal radiator with a full-wavelength sectorial director and a flat reflector, with the sketch of its surface current distributions to be depicted in Fig. 1 (a).

The flared angle of the principal dipole is set as 270° [38]. In order to determine the distance between the director and the principal radiator as well as the radius and flared angle of the director, a six-source model is developed and shown in Fig. 1 (b): Six infinitesimal, electric current sources are sampled on the peripherals of the director and principal radiator, at the antinode and half-power point of the current distribution, respectively. The combined far field of the antenna at arbitrary observation point P can be superpositioned as

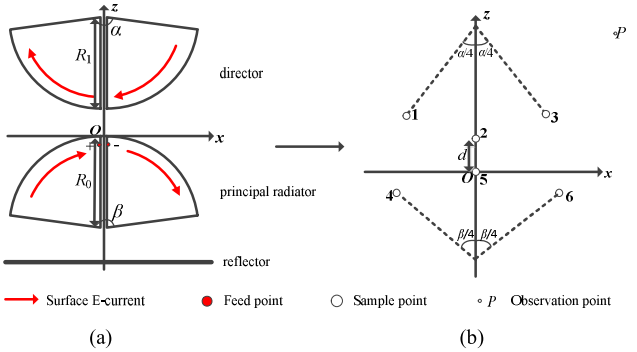

FIGURE 1. Conceptual design in preliminary, (a) schematic diagram of the conceptual antenna, and (b) a six-source model of the proposed antenna.

$$F_{(\theta,\varphi)} = E\Big\{1 + e^{j\varphi_{00}} + \Big[A_1 e^{j\varphi_{10}} + A_2 e^{j\varphi_{20}} + A_3 e^{j\varphi_{30}}\Big] + \Big[A_4 e^{j\varphi_{40}} + A_6 e^{j\varphi_{60}}\Big]\Big\} \quad (1)$$

The radiation behavior of the antenna can be accordingly functioned by $F\ (\theta, \varphi)$ shown in (1), where E is the magnitude of the E-fields, with its detailed phase shift terms presented in the Appendix. As seen from Fig. 1 (b), source 2 locates at $z = d$, source 5 is set at the origin (i.e., the phase center of the whole antenna system). The magnitudes of source 5, and the reflector are set as 1.0, while the ones of source 4 and 6 should be accordingly as $A_4 = A_6 = 0.707$, respectively. Since the director can be treated as a parasitic element, the magnitude of the electric field intensity should be smaller than unity. Therefore, the amplitude of source 2 can be reasonably set as 0.707, while the ones of source 1 and 3 should be accordingly as $A_1 = A_3 = 0.5$, respectively.

Suppose the antenna will be designed on dielectric substrate with relative permittivity of $\varepsilon_r = 2.65$ at the center frequency of 2.4 GHz. The radius and flared angle of the principal sectorial dipole can be calculated by (2) [39], where ε_e is relative dielectric constant that can be estimated by empirical expressions indicated in [40], ν is the circumferential eigen-number determined by the flared angle α, and $\chi_{\nu 1}$ is the first root of the first-order derivative of the ν-order Bessel function of the first kind, respectively [38], [39]. When the flared angle is set as $\beta = 270°$ [38], the radius can be initially calculated as $R_0 = 26.5$ mm [41].

$$R_0 = \frac{\chi_{\nu 1}}{2\pi\varepsilon_e}\lambda$$
$$\nu = \frac{\pi}{\alpha} \quad (2)$$

Secondly, let's set $\alpha = 240°$ as the initial value for the director. By using (1), the normalized directivity function can be analyzed, tuned, and plotted in Fig. 2. Radiation patterns are normalized with respect to the peak gain in each principal-cut plane. When d is tuned to $0.024\lambda_g$ (λ_g is the guided wavelength of the corresponding center frequency), the front-to-back ratio can be enhanced and the E-plane pattern can be narrowed down, with H-plane pattern rarely changed. Therefore, it is seen that a close separation of

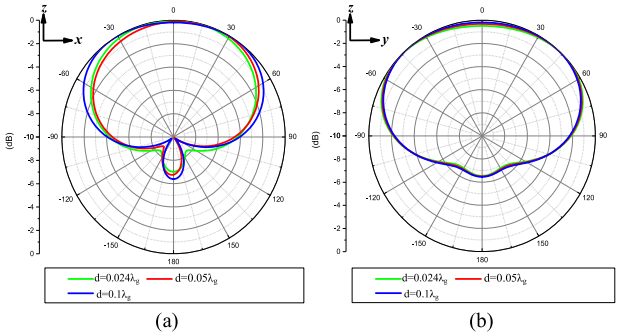

FIGURE 2. Theoretically calculated normalized radiation behavior of the proposed antenna with different d ($\alpha = 240°$), (a) zx-plane, (b) zy-plane.

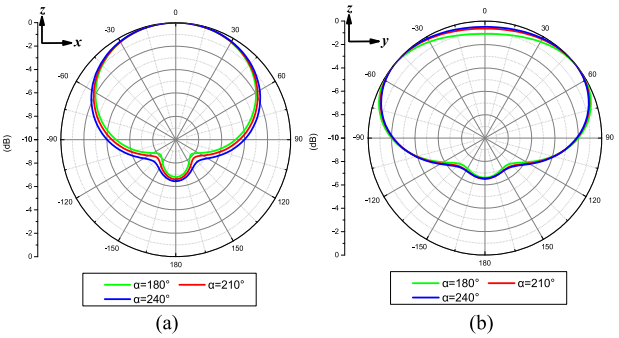

FIGURE 3. Theoretically calculated normalized radiation behavior of the proposed antenna with different $\alpha(d = 0.024\lambda_g)$, (a) zx-plane, (b) zy-plane.

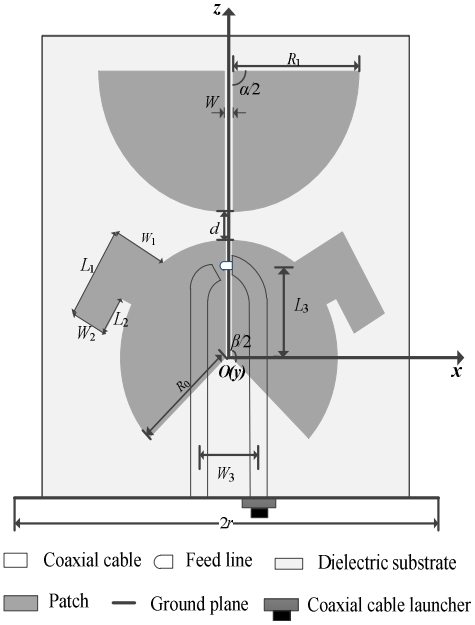

FIGURE 4. Schematic of the proposed three-element Yagi-Uda antenna.

TABLE 1. Design parameters of proposed antenna (unit: mm).

Parameters	R_0	R_1	α	β	L_1	L_2	L_3	W	W_1	W_2	W_3	r
Theoretical	26.5	32.6	180°	270°	14	6	22.8	1.6	11.3	8	8.8	62.5
Numerical	26.0	31.8										

d between principal dipole and director may be beneficial for directivity enhancement for Yagi-Uda antenna designs. Unlike the conventional cases of 0.1-wavelength to 0.3-wavelength [5], the separation can be remarkably reduced to $0.024\lambda_g$ in the case of 2-D full- wavelength sectorial case.

Then, in the other cases of $\alpha = 180°$, $210°$, $240°$, the radius of the director can be analyzed and tuned by using (1) and (2), for further directivity enhancement, which yield $R_1 = 32.6$ mm, 29.3 mm, 26.8 mm, respectively. When α is tuned to 180°, the front-to-back ratio can be improved, and the main beam can be narrowed down. Therefore, a semi-circular director with radius of 32.6 mm can be initially determined and set in the design.

Through the approximate theoretical prediction and analyses, it can be well figured out that a better directivity and narrower main beam can be simultaneously attained when the key parameters of the director set as $\alpha = 180°$, $R_1 = 32.6$ mm, and $d = 0.024\lambda_g$, respectively.

B. ANTENNA DESIGN AND PARAMETRIC STUDIES

Fig. 4 depicts the schematic of the proposed three-element PCB Yagi-Uda with a principal sectorial radiator, a circular metallic flat reflector, and a sectorial director, which will be designed herein at the center frequency of 2.4 GHz as one design example. The radius of the circular metallic flat reflector is $r = 62.5$ mm, which is approximately equal to one half-wavelength of center frequency. The dielectric constant of the dielectric substrate is 2.65, and the thickness is $h = 1$ mm. The relative dielectric constant can be approximately calculated by [40], which yields $\varepsilon_e = 1.124$.

As seen from Fig. 4, the principal radiator is symmetrically fed by an adhesive coaxial cable with a dummy cable. The outer conductor of the cable is bonded to one arm of the principal radiator, with the inner one connected to the other one [42]. To maintain the antenna's balanced configuration, a dummy cable should be attached to the other arm. A pair of open-circuited, tuning stubs with lengths of L_1, L_2 and widths of W_1, W_2 can be introduced on the periphery of the sectorial principal radiator to perturb the second odd-order resonant mode and to yield dual-resonant characteristic [38].

Parametric studies on three design parameters of W, L_3 and W_3 have been performed to validate the theoretical results by using the HFSS simulator, with the results given in Fig. 5(a) to (c). The initial design parameters of $W = 1.6$ mm, $L_3 = 22.8$ mm, $W_3 = 8.8$ mm are empirically estimated with reference to [38]. All initial parameters are given in Table 1. It can be seen that the antenna's impedance bandwidth can be finely tuned by adjusting the three parameters. In addition, the effect of the radius of reflector of r is studied. As can be seen from Fig. 5(d), the frequency response of $|S_{11}|$ is insensitive to the radius of the reflector to a certain extent. The final parameters of the antenna are tabulated in Table 1 and the key ones compared to the theoretical ones. It is seen both results agree reasonably well.

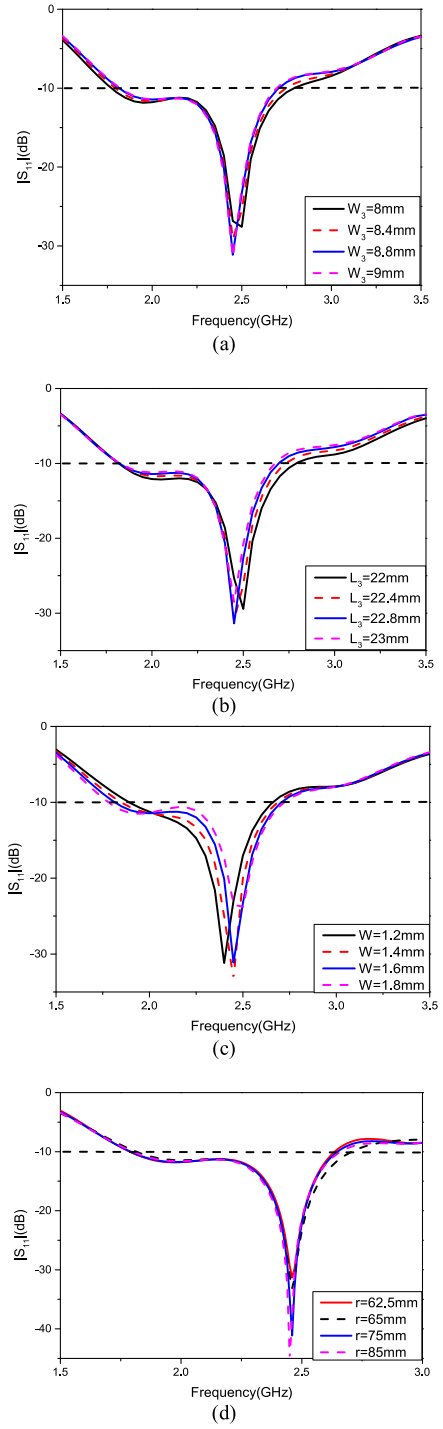

FIGURE 5. Parametric studies on the position of the feed line and the reflector, (a) W_3 ($L_3 = 22$ mm, $W = 1.6$ mm), (b) L_3 ($W_3 = 9$ mm, $W = 1.6$ mm), (c) W ($L_3 = 22$ mm, $W_3 = 9$ mm) and (d) r ($W = 1.6$ mm, $L_3 = 22.8$ mm, $W_3 = 8.8$ mm).

III. NUMERICAL AND EXPERIMENTAL VALIDATIONS

Based on the theoretical calculations and numerical simulations, a prototype antenna (Ant.1) is designed and fabricated for validation. The design approach is then validated on a modified Teflon substrate [43] with relative permittivity $\varepsilon_r = 2.65$ and thickness $h = 1$ mm, as shown in Fig. 6. The

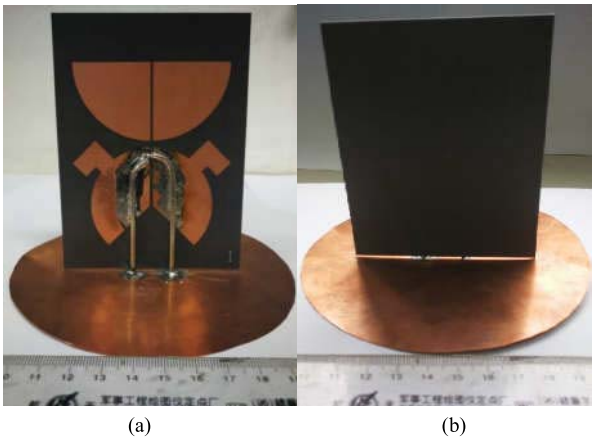

FIGURE 6. Photograph of the fabricated antenna prototype of the proposed antenna, (a) front view, (b) back view.

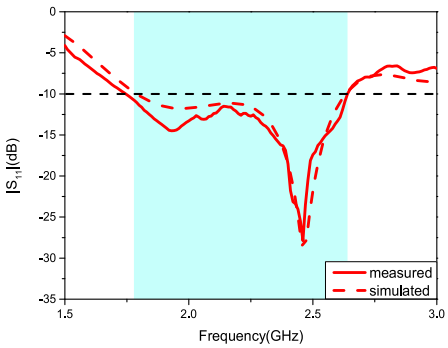

FIGURE 7. Simulated and measured reflection coefficients of Ant.1.

antenna prototype's reflection coefficient, radiation patterns, efficiency and gain are measured by employing an Agilent's N5230A vector network analyzer (VNA) and a Satimo's Starlab near-field antenna measurement system, respectively.

The simulated and measured reflection coefficients of the antenna are shown in Fig. 7 (Ant.1). It is seen that the simulated and measured reflection coefficients match very well with each other. Due to two resonances in the range of 1.79 ∼ 2.63 GHz, the fabricated antenna exhibits broadband radiation characteristics. For reflection coefficients lower than −10 dB, the measured impedance bandwidth is up to 37.1%.

Fig. 8 shows the measured and simulated normalized radiation patterns in zx-plane and zy-plane at different resonant frequencies (1.93 GHz, 2.46 GHz) of the Ant.1. It is able to be seen that all measured patterns match well with the simulated ones. Moreover, the measured cross-polarization levels within both principal-cut planes are lower than −20 dB, which implies the antenna should exhibit good polarization purity.

The simulated and measured bore-sight (i.e., $+z$-direction) radiation gains are plotted in Fig. 9. It can be seen that the measured gain is in good agreement with the simulated gain in the whole impedance bandwidth with discrepancy less than 0.7 dB. Furthermore, it is clearly seen from Fig. 9 that the in-band gain fluctuation does not exceed 2.1 dB, which

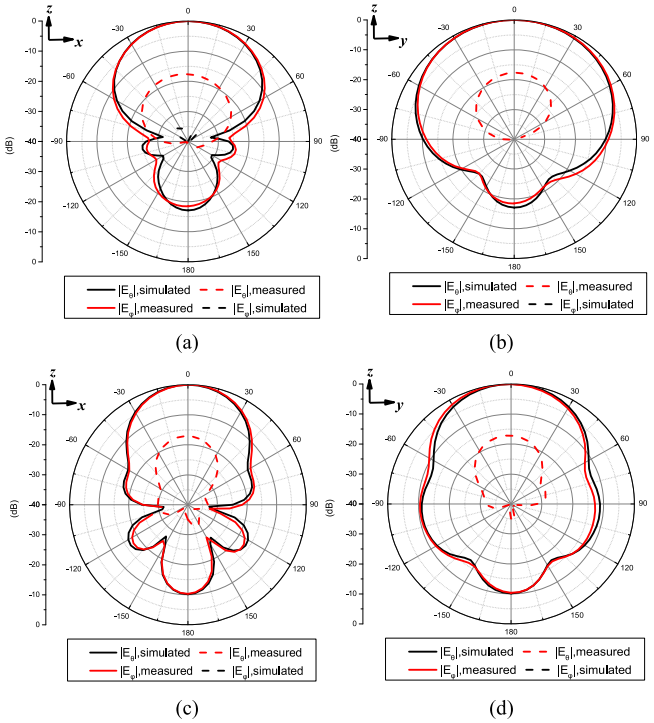

FIGURE 8. Simulated and measured results of the normalized radiation behaviors of Ant.1 at different frequencies, (a) and (b) *zx*- and *zy*-plane at 1.93 GHz, (c) and (d) *zx*- and *zy*-plane at 2.46 GHz.

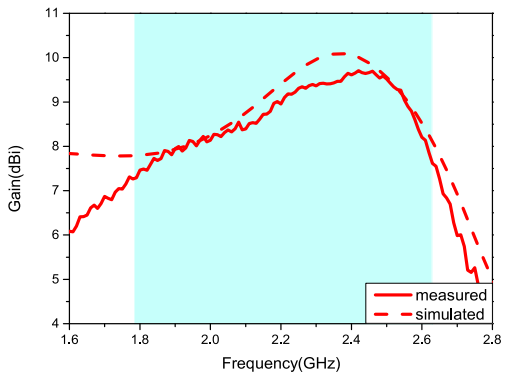

FIGURE 9. Simulated and measured gain variation of Ant.1.

indicates that gain variation should be relatively flat. In addition, the maximum gain of the simulated antenna is up to 10.1 dBi, and the average in-band gain also reaches to 9.0 dBi. The measured maximum and average gains are 9.6 dBi and 8.5 dBi, respectively, which match well with the simulated ones. For the traditional three-element Yagi-Uda antenna, the maximum gain is generally about 7.5 dBi [5]. It can be clearly seen that the presented design approach can effectively improve the gain and realize a wide bandwidth in simultaneous way.

Without loss of generality, two kinds of Yagi-Uda antennas with different directors having flared angle of 210° and 240° (Ant. 1a and Ant.1b) are further designed, manufactured, and measured to verify the validity of the design approach. Let's

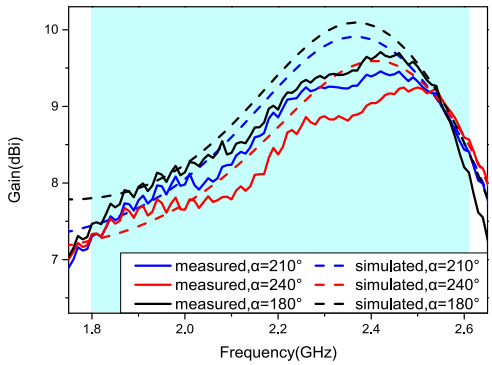

FIGURE 10. Simulated and measured radiation gains for Ant.1, Ant.1a and Ant.1b ($d = 0.024\lambda_g$).

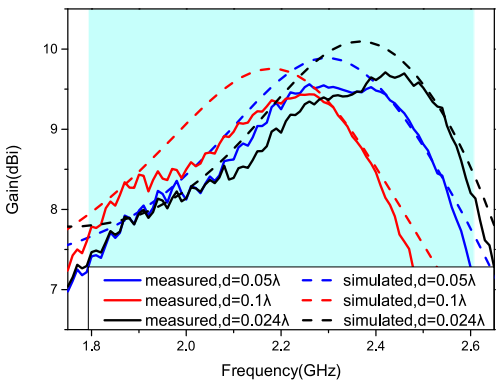

FIGURE 11. Simulated and measured radiation gains for Ant.1, Ant.1c and Ant.1d ($\alpha = 180°$).

set $d = 0.024\lambda_g$ as the initial value for the distance between the principal radiator and the director. Fig. 10 shows the bore-sight simulated and measured radiation gains for the antenna having a director with different flared angles of $\alpha = 180°$, $\alpha = 210°$, and $\alpha = 240°$, respectively.

As can be seen from Fig. 10, all measured bore-sight gains agree well with the simulated ones. The in-band gain fluctuation of all antennas does not exceed 2.5 dB, which indicates that the gain fluctuation of such type of antennas should be relatively stable. The maximum gains in the cases of $\alpha = 210°$ and $\alpha = 240°$ are 9.9 dBi and 9.6 dBi, respectively, which are inferior to 10.1 dBi in the case of $\alpha = 180°$.

Next, let's come to study the effect of separation d of the dipole and the director. Two antennas (Ant. 1c and Ant. 1d) with $d = 0.05\lambda_g$ and $d = 0.1\lambda_g$ between the principal radiator and the director are designed to verify the predicted results. Set $\alpha = 180°$ as the flared angle of the director. Fig. 11 shows the simulated and measured radiation gains for $d = 0.05\lambda_g$, $d = 0.1\lambda_g$, and $d = 0.024\lambda_g$.

As seen from Fig. 11, the simulated and measured bore-sight gains match well with each other, the variation in gain is still stable. The maximum gains at the distances of $0.05\lambda_g$ and $0.1\ \lambda_g$ are 9.8 dBi and 9.7 dBi, respectively, which are inferior to the $0.024\lambda_g$ ones. It proves that narrow distance

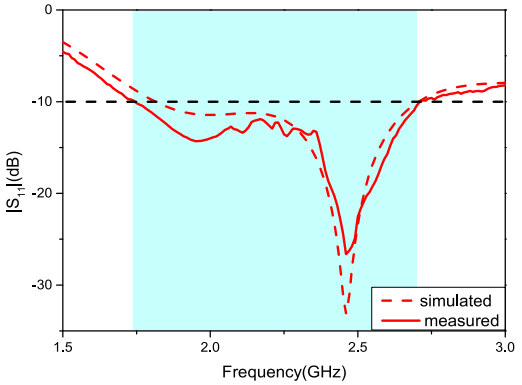

FIGURE 12. Simulated and measured reflection coefficients of Ant.2.

can lead to better performance, and can also validate the predicted results. These further validations evidently convince the correctness and effectiveness of the design approach based on the simplified multi-point equivalent source model presented in Section II-A.

Further studies have been carried out to enhance the antenna gain. The gain can be further improved by setting the length of the reflector to about $1.3\lambda_g$ [6], [44]. For comparisons, the length of the reflector is modified to $1.36\lambda_g$ ($r = 85$ mm), with other parameters in Table 1 unchanged. This yields the design of Ant.2.

Fig. 12 depicts the simulated and measured reflection coefficients of Ant.2. The simulated and measured reflection coefficients agree well, and the fabricated antenna still shows a dual-resonant wideband characteristic from 1.81 to 2.7 GHz, with an impedance bandwidth for $|S_{11}| < -10$ dB of 39.5%.

Fig. 13 exhibits the measured normalized radiation patterns in comparison with the simulated ones. It is observed that all the measured radiation patterns are in good agreement with the simulated ones. In particular, in most of frequency ranges, the simulated cross-polarization levels are lower than -40 dB and the measured one are lower than -25 dB. The cross-polarization components are caused by fabrication tolerance of the prototype and unpredicted imperfectness (i.e., loss and surface roughness, etc.) of the materials. This implies a larger reflector should be beneficial for polarization purity enhancement, compared to Ant.1.

The simulated and measured bore-sight radiation gains and efficiencies of Ant.2 are plotted in Fig. 14. As seen, both the simulated and measured efficiencies within the impedance bandwidth exceed 90%. The simulated and measured peak gains reach to as high as 10.8 dBi and 10.4 dBi, and the average gains are 9.5 dBi and 9.4 dBi, respectively. The in-band gain fluctuation does not exceed 3.0 dB, while maintaining its bandwidth of nearly 40%.

Table 2 tabulates a comprehensive comparison with other reported Yagi-Uda antennas [6]–[7], [10]–[11], [31], [45]–[48], in terms of the number of elements, type of the principal radiator, impedance bandwidth, peak gain and

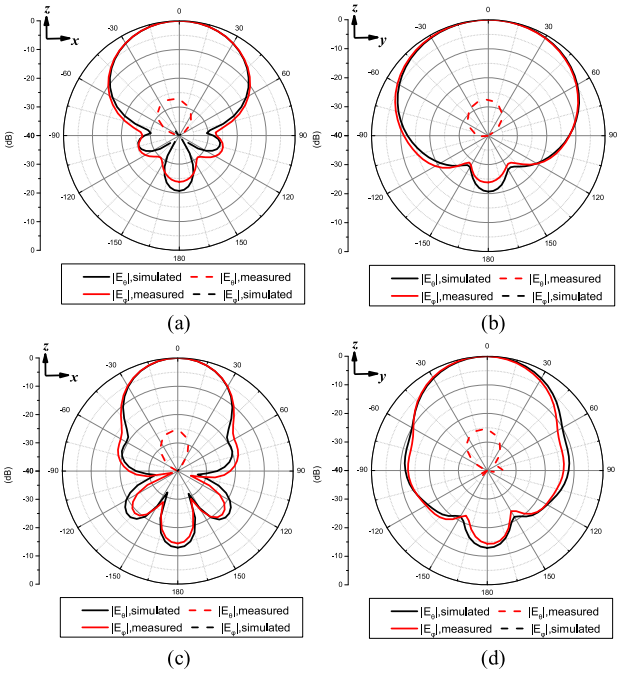

FIGURE 13. Simulated and measured results of the normalized radiation patterns of Ant.2 at different frequencies, (a) and (b) *zx*- and *zy*-plane at 1.93 GHz, (c) and (d) *zx*- and *zy*-plane at 2.46 GHz.

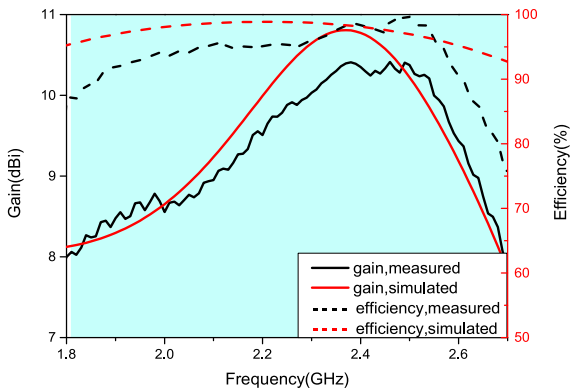

FIGURE 14. Simulated and measured radiation gains and efficiencies of Ant.2.

peak realized gain. It is shown that the proposed antenna is unique, in terms of its 2-D, full-wavelength dipole configuration. In addition, the proposed antenna has a 39.5% impedance bandwidth and the measured maximum gain is up to 10.4 dBi, while maintaining a simple design. Compared to the high gain counterparts [6], [11], [48], the advanced antenna exhibits wider bandwidth, simpler configuration, and comparable gain. The gain of the advanced antenna is about 3.0 dB superior to the conventional wideband, three-element counterparts [10], [31], [45]–[47], and even about 1.0 dB higher than the four-element one [7]. By comparison, it is seen that the proposed antenna can maintain a relatively small size while maintaining a high gain [7], [45]–[48]. In general, the proposed antenna has exhibited its superior performance and lower configurational complexity to most

TABLE 2. Yagi-Uda antennas for comparisons (N.A. = not available).

Reference	Number of Elements	Principal radiator	Size (λ_g*λ_g)	Impedance Bandwidth	Peak Realized Gain (dBi)
6	3	1.5-wavelength	N.A.	N.A.	11.5
7	4	Half-wavelength	2.34*2.34	66%	9.5
10	3	Half-wavelength	0.5*0.5	48%	6.5
11	3	Half-wavelength	N.A.	12.44%	10.3
32	3	Half-wavelength	1.56*1.52	92.2%	6
46	3	Half-wavelength	0.28*0.23	41.5%	5.5
47	3	Half-wavelength	1.3*1.47	96.4%	6.8
48	3	Half-wavelength	0.24*0.24	69.1%	4.1
49	3	Half-wavelength	1.2*1.2	17.6%	10
This work	**3**	**Full-wavelength**	**0.48*0.69**	**39.5%**	**10.4**

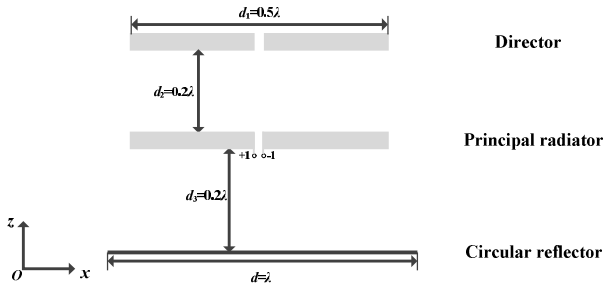

FIGURE 15. Schematic of traditional Yagi-Uda antenna (Ant.1.1).

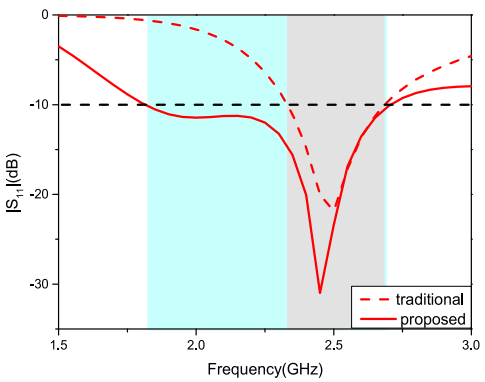

FIGURE 16. Simulated reflection coefficients of Ant.1.1 and proposed antenna.

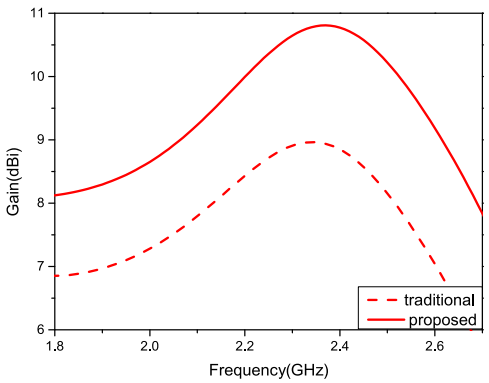

FIGURE 17. Simulated gain variation of Ant.1.1 and proposed antenna.

of the existing Yagi-Uda antennas, while realizing wideband, high gain and maintaining simple configuration.

Without loss of generality, an example of classical Yagi-Uda antenna having linear, half-wavelength dipole radiator and director above the conductive circular disk reflector has been added for comparison. In Fig. 15, the three-element Yagi-Uda antenna under comparison (Ant.1.1) uses an identical flat, circular reflector. The distance between the reflector and principal radiator is $0.2\lambda_g$, and the distance between the principal radiator and the director is also $0.2\lambda_g$, as conventional Yagi-Uda antennas [5] behave. The simulated reflection coefficients of Ant.1.1 and proposed antenna are shown in Fig. 16. It is seen that the bandwidth of Ant.1.1 is about 14.5%, while that of the proposed antenna is enlarged up to 39.5%, i.e., nearly triple of the traditional one. Fig. 17 exhibits the simulated gain frequency responses of Ant.1.1 and the advanced antenna. It is seen that the peak gain of the traditional Yagi-Uda antenna is 8.8 dBi, which is about 1.6 dB lower than that of the advanced one's. By comparisons, the advanced 2-D sectorial configuration would

be more promising for high gain Yagi-Uda antenna designs without significantly increasing the size.

IV. CONCLUSION

In this paper, a novel design approach to a wideband closely-spaced, three-element Yagi-Uda antenna is advanced. The advanced antenna is designed based upon a unique 2-D, full-wavelength dipole configuration. Unlike the conventional Yagi-Uda antennas based on half-wavelength dipoles, the director of the novel antenna can be coupled in a close proximity to the principal dipole through a separation of 0.024- wavelength, which yields a high gain characteristic of over 10 dBi. As validated, the proposed antenna can exhibit an impedance bandwidth up to about 40%, with in-band maximum gain up to 10.4 dBi and gain fluctuation less than 3 dB. It has been verified that the designed antenna can cover a variety of wireless spectra such as 5-G mobile communications (2.6 GHz), TD-LTE (2.37-2.66 GHz), WLAN (2.4-2.5 GHz), etc. Moreover, the advanced Yagi-Uda antenna has been extensively investigated and discussed to reveal its attractive advantages of high gain, wide band, simple structure and easy fabrication. As a consequence, this antenna can be applied as a promising high gain antenna for future broadband wireless applications.

APPENDIX

In the multi-source model, the array factor is dependent on the spatial and temporal phase shift terms, which can be calculated according to the geometrical relationship. The spatial and temporal phase shift terms of φ_{00}, φ_{10}, φ_{20}, φ_{30}, φ_{40}, and φ_{60} in (1) can be depicted in detail by

$$\varphi_{00} = -kl\cos\theta + \pi/2 \tag{A.1}$$
$$\varphi_{10} = -kd_x\sin\theta\cos\varphi + kd_z\cos\theta \tag{A.2}$$
$$\varphi_{20} = kd\cos\theta \tag{A.3}$$
$$\varphi_{30} = kd_x\sin\theta\cos\varphi + kd_z\cos\theta \tag{A.4}$$
$$\varphi_{40} = -kd'_x\sin\theta\cos\varphi + kd'_z\cos\theta \tag{A.5}$$
$$\varphi_{60} = kd'_x\sin\theta\cos\varphi + kd'_z\cos\theta \tag{A.6}$$
$$d_x = R_0\sin(\alpha/4) \tag{A.7}$$
$$d'_x = R_1\sin(\beta/4) \tag{A.8}$$
$$d_z = d + R_0[1-\cos(\alpha/4)] \tag{A.9}$$
$$d'_z = R_1[1-\cos(\beta/4)] \tag{A.10}$$

where φ_{00} is the total phase of the reflector contributed by the spatial phase shift and the temporal one of $\pi/2$, $k = 2\pi/\lambda$ is the wavenumber, λ is the free-space wavelength, R_0 is the radius of the director, R_1 is the radius of the principal radiator, l is the separation between the reflector from the origin of the coordinates, α and β are the flared angles of the director and the principal radiator, θ and φ are elevation angle and azimuth angle, respectively. A more intuitive six-source model is shown in Fig. A1.

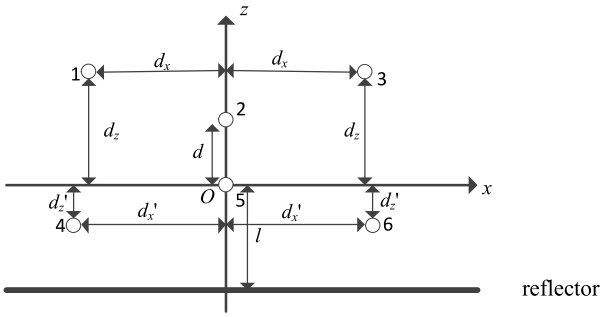

FIGURE A1. A clear six-source model of the proposed antenna.

ACKNOWLEDGMENT

The authors are grateful to Xiu-Qiong Xing and Xiao-Hui Mao for their beneficial suggestions and warm encouragement, and also grateful to the anonymous reviewers for their beneficial comments and suggestions on this article.

REFERENCES

[1] H. Yagi, "Beam transmission of ultra short waves," *Proc. Inst. Radio Eng.*, vol. 16, no. 6, pp. 715–740, Jun. 1928.
[2] C. Lee and L.-C. Shen, "Coupled Yagi arrays," *IEEE Trans. Antennas Propag.*, vol. 25, no. 6, pp. 889–891, Nov. 1977.
[3] S. Lim and H. Ling, "Design of a closely spaced, folded Yagi antenna," *IEEE Antennas Wireless Propag. Lett.*, vol. 5, pp. 302–305, 2006.
[4] S. Lim and M. F. Iskander, "Design of a dual-band, compact Yagi antenna over an EBG ground plane," *IEEE Antennas Wireless Propag. Lett.*, vol. 8, pp. 88–91, 2009.
[5] C. Chen and D. Cheng, "Optimum element lengths for Yagi-Uda arrays," *IEEE Trans. Antennas Propag.*, vol. 23, no. 1, pp. 8–15, Jan. 1975.
[6] F. Landstorfer, "A new type of directional antenna," in *Proc. Antennas Propag. Soc. Int. Symp.*, Amherst, MA, USA, 1976, pp. 169–172.
[7] S. I. H. Shah and S. Lim, "High gain Yagi-Uda origami antenna," in *Proc. Int. Symp. Antennas Propag. (ISAP)*, 2016, pp. 388–389.
[8] Y. Luo and Q.-X. Chu, "A Yagi–Uda antenna with a stepped-width reflector shorter than the driven element," *IEEE Antennas Wireless Propag. Lett.*, vol. 15, pp. 564–567, 2016.
[9] E. Huang and T. Chiu, "Printed Yagi antenna with multiple reflectors," *Electron. Lett.*, vol. 40, no. 19, pp. 1165–1166, Sep. 2004
[10] N. Kaneda, W. R. Deal, Y. X. Qian, R. Waterhouse, and T. Itoh, "A broadband planar quasi-Yagi antenna," *IEEE Trans. Antennas Propag.*, vol. 50, no. 8, pp. 1158–1160, Aug. 2002.
[11] D. Arceo and C. A. Balanis, "A compact Yagi–Uda antenna with enhanced bandwidth," *IEEE Antennas Wireless Propag. Lett.*, vol. 10, pp. 442–445, 2011.
[12] J. K. Yu and S. Lim, "A multi-band, closely spaced Yagi antenna with helical-shaped directors," in *Proc. IEEE Antennas Propag. Soc. Int. Symp.*, 2009, pp. 1–4.
[13] S. Lim, "Design of a multidirectional, high-gain compact Yagi antenna," *IEEE Antennas Wireless Propag. Lett.*, vol. 8, pp. 418–420, 2009.
[14] S. Lim and H. Ling, "Design of electrically small Yagi antenna," *Electron. Lett.*, vol. 43, no. 5, pp. 3–4, 2007.
[15] R. Bhattacharya, R. Garg, and T. K. Bhattacharyya, "A compact Yagi–Uda type pattern diversity antenna driven by CPW-fed pseudomonopole," *IEEE Trans. Antennas Propag.*, vol. 64, no. 1, pp. 25–32, Jan. 2016.
[16] J. Huang and A. C. Demission, "Microstrip Yagi array antenna for mobile satellite vehicle application," *IEEE Trans. Antennas Propag.*, vol. 39, no. 7, pp. 1024–1030, Jul. 1991.
[17] O. Kramer, T. Djerafi, and K. Wu, "Very small footprint 60 GHz stacked Yagi antenna array," *IEEE Trans. Antennas Propag.*, vol. 59, no. 9, pp. 3204–3210, Sep. 2011

[18] Z. Briqech, A. R. Sebak, and T. A. Denidni, "High-efficiency 60-GHz printed Yagi antenna array," *IEEE Antennas Wireless Propag. Lett.*, vol. 12, pp. 1224–1227, 2013.
[19] W. Zhou, J. Liu, and Y. Long, "A broadband and high-gain planar complementary Yagi array antenna with circular polarization," *IEEE Trans. Antennas Propag.*, vol. 65, no. 3, pp. 1446–1451, Mar. 2017.
[20] D. Gray, J. W. Lu, and D. V. Thiel, "Electronically steerable Yagi–Uda microstrip patch antenna array," *IEEE Trans. Antennas Propag.*, vol. 46, no. 5, pp. 605–608, May 1998.
[21] P. R. Grajek, B. Schoenlinner, and G. M. Rebeiz, "A 24-GHz high-gain Yagi-Uda antenna array," *IEEE Trans. Antennas Propag.*, vol. 52, no. 5, pp. 1257–1261, May 2004.
[22] M. Khodier and M. Al-Aqil, "Design and optimisation of Yagi-Uda antenna arrays," *IET Microw. Antennas Propag.*, vol. 4, no. 4, pp. 426–436, Apr. 2010.
[23] Q. Xin, F. Zhang, B. Sun, Y. Zou, and Q. Liu, "Yagi-Uda antenna with small size for vehicles," *Electron. Lett.*, vol. 47, no. 7, pp. 428–430, 2011.
[24] R. A. Alhalabi and G. M. Rebeiz, "High-gain Yagi-Uda antennas for millimeter-wave switched-beam systems," *IEEE Trans. Antennas Propag.*, vol. 57, no. 11, pp. 3672–3676, Nov. 2009.
[25] R. A. Alhalabi and G. M. Rebeiz, "Differentially-fed millimeter-wave Yagi-Uda antennas with folded dipole feed," *IEEE Trans. Antennas Propag.*, vol. 58, no. 3, pp. 966–969, Mar. 2010.
[26] H. Chu, Y. Guo, H. Wong, and X. Shi, "Wideband self-complementary quasi-Yagi antenna for millimeter-wave systems," *IEEE Antennas Wireless Propag. Lett.*, vol. 10, pp. 322–325, 2011.
[27] P. Cheong, K. Wu, W. Choi, and K. Tam, "Yagi–Uda antenna for multiband radar applications," *IEEE Antennas Wireless Propag. Lett.*, vol. 13, pp. 1065–1068, 2014.
[28] O. M. Khan, Z. U. Islam, Q. U. Islam, and F. A. Bhatti, "Multiband high-gain printed Yagi array using square spiral ring metamaterial structures for S-band applications," *IEEE Antennas Wireless Propag. Lett.*, vol. 13, pp. 1100–1103, 2014.
[29] S. A. Alekseytsev and A. P. Gorbachev, "The novel printed dual-band quasi-Yagi antenna with end-fed dipole-like driver," *IEEE Trans. Antennas Propag.*, vol. 68, no. 5, pp. 4088–4090, May 2020.
[30] Y. Cai, Y. J. Guo, and P.-Y. Qin, "Frequency switchable printed Yagi-Uda dipole sub-array for base station antennas," *IEEE Trans. Antennas Propag.*, vol. 60, no. 3, pp. 1639–1642, Mar. 2012.
[31] J. Wu, Z. Zhao, Z. Nie, and Q.-H. Liu, "Design of a wideband planar printed quasi-Yagi antenna using stepped connection structure," *IEEE Trans. Antennas Propag.*, vol. 62, no. 6, pp. 3431–3435, Jun. 2014.
[32] G. Zheng, A. A. Kishk, A. W. Glisson, and A. B. Yakovlev, "Simplified feed for modified printed Yagi antenna," *Electron. Lett.*, vol. 40, no. 8, pp. 464–466, 2004.
[33] Y.-W. Hsu, T.-C. Huang, H.-S. Lin, and Y.-C. Lin, "Dual-polarized quasi Yagi–Uda antennas with endfire radiation for millimeter-wave MIMO terminals," *IEEE Trans. Antennas Propag.*, vol. 65, no. 12, pp. 6282–6289, Dec. 2017.
[34] A. Abbosh, "Ultra-wideband quasi-Yagi antenna using dual-resonant driver and integrated balun of stepped impedance coupled structure," *IEEE Trans. Antennas Propag.*, vol. 61, no. 7, pp. 3885–3888, Jul. 2013.
[35] W.-J. Lu, X.-Q. Li, Q. Li, and L. Zhu, "Generalized design approach to compact wideband multi-resonant patch antennas," *Int. J. RF Microw. Comput. Aided Eng.*, vol. 28, no. 8, Aug. 2018, Art. no. e21481.
[36] C. Ding, B. Jones, Y. J. Guo, and P.-Y. Qin, "Wideband matching of full-wavelength dipole with reflector for base station," *IEEE Trans. Antennas Propag.*, vol. 65, no. 10, pp. 5571–5576, Oct. 2017.
[37] C. Ding, H.-H. Sun, H. Zhu, and Y. J. Guo, "Achieving wider bandwidth with full-wavelength dipoles (FWDs) for 5G base stations," *IEEE Trans. Antennas Propag.*, vol. 68, no. 2, pp. 1119–1127, Feb. 2020.
[38] Z.-B. Zhao, W.-J. Lu, L. Zhu, and J. Yu, "Wideband wide beamwidth full-wavelength sectorial dipole antenna under dual-mode resonance," *IEEE Trans. Antennas Propag.*, vol. 69, no. 1, pp. 14–24, Jan. 2021.
[39] W. Richards, J.-D. Ou, and S. A. Long, "A theoretical and experimental investigation of annular, annular sector, and circular sectormicrostrip antennas," *IEEE Trans. Antennas Propag.*, vol. 32, no. 8, pp. 864–867, Aug. 1984.
[40] R. Janaswamy and D. H. Schaubert, "Characteristic impedance of a wide slotline on low-permittivity substrates," *IEEE Trans. Microw. Theory Techn.*, vol. 34, no. 8, pp. 900–902, Aug. 1986.
[41] W.-J. Lu, Q. Li, S.-G. Wang, and L. Zhu, "Design approach to a novel dual mode wideband circular sector patch antenna," *IEEE Trans. Antennas Propag.*, vol. 65, no. 10, pp. 4980–4990, Oct. 2017.
[42] W. J. Lu, L. Zhu, K. W. Tam, and H. B. Zhu, "Wideband dipole antenna using multi-mode resonance concept," *Int. J. Microw. Wireless Technol.*, vol. 9, no. 2, pp. 365–371, 2017.
[43] Accessed: Oct. 24, 2017. [Online]. Available: http://www.wang-ling.com.cn/products_view.asp?id=484
[44] J. D. Kraus, *Antennas*, 2nd ed. New York, NY, USA: McGraw-Hill, 1988.
[45] S. A. Rezaeieh, M. A. Antoniades, and A. M. Abbosh, "Miniaturized planar Yagi antenna utilizing capacitively coupled folded reflector," *IEEE Antennas Wireless Propag. Lett.*, vol. 16, pp. 1977–1980, 2017.
[46] J. Wu, Z. Zhao, Z. Nie, and Q. Liu, "Bandwidth enhancement of a planar printed quasi-Yagi antenna with size reduction," *IEEE Trans. Antennas Propag.*, vol. 62, no. 1, pp. 463–467, Jan. 2014.
[47] S. A. Rezaeieh, M. A. Antoniades, and A. M. Abbosh, "Miniaturization of planar Yagi antennas using mu-negative metamaterial-loaded reflector," *IEEE Trans. Antennas Propag.*, vol. 65, no. 12, pp. 6827–6837, Dec. 2017.
[48] Z. Liang, J. Liu, Y. Zhang, and Y. Long, "A novel microstrip quasi Yagi array antenna with annular sector directors," *IEEE Trans. Antennas Propag.*, vol. 63, no. 10, pp. 4524–4529, Oct. 2015.

WEN-QI JIA was born in Shijiazhuang, Hebei, China, in 1996. He received the B.Sc. degree in communication engineering from Southwest Minzu University, Chengdu, China, in 2018. He is currently pursuing the M.E. degree with the Nanjing University of Posts and Telecommunications, Nanjing, China. His recent research interests include antennas theory and antennas design approach.

FEI-YAN JI was born in Taizhou, Jiangsu, China, in 1997. She received the B.E. degree in communication engineering from Jiangnan University, Wuxi, China, in 2019. She is currently pursuing the M.E. degree with the Nanjing University of Posts and Telecommunications, Nanjing, China. Her recent research interests include the complementary dipole antennas theory and design approach.

WEN-JUN LU (Senior Member, IEEE) was born in Jiangmen, Guangdong, China, in 1978. He received the Ph.D. degree in electronic engineering from the Nanjing University of Posts and Telecommunications, Nanjing, China, in 2007, where he has been a Professor with the Jiangsu Key Laboratory of Wireless Communications since 2013. From 2015 to 2016, he invented the design approach to planar endfire circularly polarized antennas. He has re-discovered the concept of 1-D multiresonant dipoles and advanced the multiresonant design approach to elementary antennas. He is the Translator of the Chinese version *The Art and Science of Ultrawideband Antennas* (by H. Schantz). He has authored two books, *Antennas: Concise Theory, Design and Applications* (in Chinese, 2014), and *Concise Antennas* (in Chinese, 2nd ed., 2020). He has authored or coauthored over 200 technical papers published in peer-reviewed international journals and conference proceedings. His research interests include antenna theory, antenna design, antenna arrays, and wireless propagation channel modeling. He was a recipient of the Exceptional Reviewers Award of the IEEE TRANSACTIONS ON ANTENNAS AND PROPAGATION in 2016 and 2020, and the Outstanding Reviewers Award of the *AEÜ: International Journal of Electronics and Communications* in 2018. He has been serving as an Editorial Board Member for the *International Journal of RF and Microwave Computer-Aided Engineering* since 2014, and an Associate Editor for the *Electronics Letters* since 2019. He is a Senior Member of Chinese Institute of Electronics (CIE), and he is a Committee Member of Antennas Society of CIE.

CHEN-XIN PAN was born in Anlu, Hubei, China, in 1996. He received the B.E. degree in communication engineering from China Three Gorges University, Yichang, China, in 2019. He is currently pursuing the M.E. degree with the Nanjing University of Posts and Telecommunications, Nanjing, China. His recent research interests include antennas theory and antenna design approach.

LEI ZHU (Fellow, IEEE) received the B.Eng. and M.Eng. degrees in radio engineering from the Nanjing Institute of Technology (currently, Southeast University), Nanjing, China, in 1985 and 1988, respectively, and the Ph.D. degree in electronic engineering from the University of Electro-Communications, Tokyo, Japan, in 1993. From 1993 to 1996, he was a Research Engineer with Matsushita–Kotobuki Electronics Industries Ltd., Tokyo. From 1996 to 2000, he was a Research Fellow with the École Polytechnique de Montréal, Montréal, QC, Canada. From 2000 to 2013, he was an Associate Professor with the School of Electrical and Electronic Engineering, Nanyang Technological University, Singapore. He joined the Faculty of Science and Technology, University of Macau, Macau, China, as a Full Professor in August 2013, and has been a Distinguished Professor since December 2016. From August 2014 to August 2017, he served as the Head of the Department of Electrical and Computer Engineering, University of Macau. He has authored or coauthored more than 650 papers in international journals and conference proceedings. His papers have been cited more than 11 500 times with the H-index of 54 (source: Scopus). His research interests include microwave circuits, antennas, periodic structures, and computational electromagnetics. He was the recipient of the 1997 Asia–Pacific Microwave Prize Award, the 1996 Silver Award of Excellent Invention from Matsushita–Kotobuki Electronics Industries Ltd., the 1993 Achievement Award in Science and Technology (First Prize) from the National Education Committee of China, the 2020 FST Research Excellence Award from the University of Macau, and the 2020 Macao Natural Science Award (Second Prize) from the Science and Technology Development Fund, Macau. He was an Associate Editor of the IEEE TRANSACTIONS ON MICROWAVE THEORY AND TECHNIQUES (2010–2013) and IEEE MICROWAVE AND WIRELESS COMPONENTS LETTERS (2006–2012). He served as a General Chair of the 2008 IEEE MTT-S International Microwave Workshop Series on the Art of Miniaturizing RF and Microwave Passive Components, Chengdu, China, and a Technical Program Committee Co-Chair of the 2009 Asia–Pacific Microwave Conference, Singapore. He served as the Member of IEEE MTT-S Fellow Evaluation Committee (2013–2015), and an IEEE AP-S Fellows Committee (2015–2017).